Accepted Manuscript

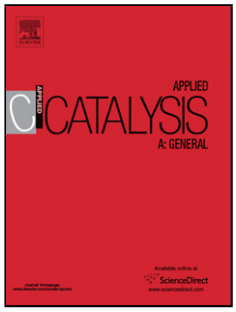

Title: Synthesis of palladium nanoparticles over graphite oxide and carbon nanotubes by reduction in ethylene glycol and their catalytic performance on the chemoselective hydrogenation of *para*-chloronitrobenzene.

Author: A.B. Dongil L. Pastor-Pérez J.L.G. Fierro N. Escalona A. Sepúlveda-Escribano

PII: S0926-860X(15)30313-6
DOI: http://dx.doi.org/doi:10.1016/j.apcata.2015.11.048
Reference: APCATA 15711

To appear in: *Applied Catalysis A: General*

Received date: 6-10-2015
Revised date: 25-11-2015
Accepted date: 27-11-2015

Please cite this article as: A.B.Dongil, L.Pastor-Pérez, J.L.G.Fierro, N.Escalona, A.Sepúlveda-Escribano, Synthesis of palladium nanoparticles over graphite oxide and carbon nanotubes by reduction in ethylene glycol and their catalytic performance on the chemoselective hydrogenation of para-chloronitrobenzene., Applied Catalysis A, General http://dx.doi.org/10.1016/j.apcata.2015.11.048

Synthesis of palladium nanoparticles over graphite oxide and carbon nanotubes by reduction in ethylene glycol and their catalytic performance on the chemoselective hydrogenation of para-chloronitrobenzene.

A.B. Dongil [*a], L. Pastor-Pérez[b], J.L.G. Fierro[c], N. Escalona[d,e], A. Sepúlveda-Escribano[b]

[a] *Universidad de Concepción, departamento de físicoquímica, laboratorio de catálisis por metales, Edmundo Larenas 129, Concepción, Chile.*

[b] *Laboratorio de Materiales Avanzados, Departamento de Química Inorgánica-Instituto Universitario de Materiales de Alicante, Universidad de Alicante, Apartado 99, E-03080 Alicante, Spain*

[c] *Instituto de Catálisis y Petroleoquímica CSIC, Grupo de Energía y Química Sostenible, C/Marie Curie2, Cantoblanco, Madrid, Spain*

[d] *Departamento de Ingeniera Química y Bioprocesos, Pontificia Universidad Católica de Chile, Avda. Vicuña Mackenna 4860, Macul, Santiago, Chile.*

[e] *Facultad de Ciencias Químicas, Pontificia Universidad Católica de Chile.*

(*) corresponding author: adongil@udec.cl

Graphical abstract

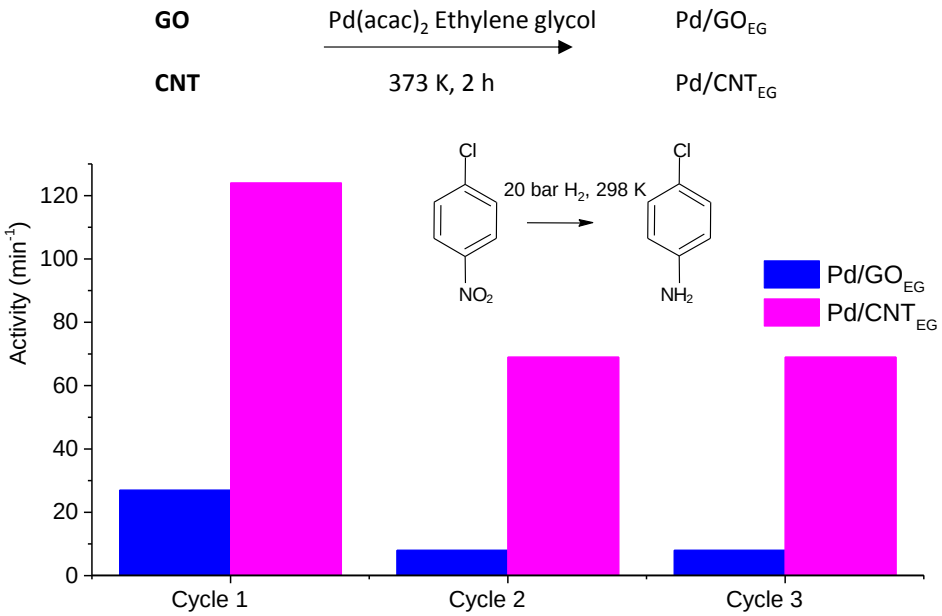

Highlights

- The synthesis of palladium nanoparticles by reduction of the organometallic precursor Pd $(acac)_2$ with ethylene glycol and their deposition over carbon nanotubes (CNT) and graphite oxide (GO) was studied.
- Well-dispersed metallic palladium nanoparticles of similar average size were obtained over Pd/CNT_{EG} and Pd/GO_{EG}, this suggesting that the morphology and surface chemistry do not affect the size of the nanoparticles obtained by this methodology
- The catalytic performance of Pd/CNT_{EG} and Pd/GO_{EG} was studied on the para-chloronitrobenzene chemoselective hydrogenation and compared with analogous catalysts prepared by traditional impregnation.
- The activity of Pd/CNT_{EG} and Pd/GO_{EG} was higher than that obtained with the catalysts prepared by impregnation and both catalysts could be reused on successive cycles.

ABSTRACT

Pd nanoparticles have been synthetized over carbon nanotubes (CNT) and graphite oxide (GO) by reduction with ethylene glycol and by conventional impregnation method. The catalysts were tested on the chemoselective hydrogenation of p-chloronitrobenzene and the effect of the synthesis method and surface chemistry on their catalytic performance was evaluated. The catalysts were characterized by N_2 adsorption/desorption isotherms at 77 K, TEM, powder X-ray diffraction, thermogravimetry, infrared and X-ray photoelectron spectroscopy and ICP-OES. It was observed that the synthesis of Pd nanoparticles employing ethylene glycol resulted in metallic palladium particles of smaller size compared to those prepared by the impregnation method and similar for both supports. The presence of oxygen groups on the support surface favored the activity and diminished the selectivity. It seems that ethylene glycol reacted with the surface groups of GO, this favoring the selectivity. The activity was higher over the CNT-based catalysts and both catalysts prepared by reduction in ethylene glycol were quite stable upon recycling.

Keywords: Carbon nanotubes; graphite oxide; palladium; ethylene glycol; para-chloronitrobenzene; hydrogenation.

1. INTRODUCTION

The interest in heterogeneous catalysts being palladium the active phase has increased recently because of its lower price and better resistance to deactivation compared to platinum, among other reasons [1-2]. However, the conventional methods to obtain supported nanoparticles for catalytic applications do not offer good metal dispersion, and alternative methods as the colloidal route have been developed. It consists on the dispersion

of the metal precursor into an appropriate solution to which the reducing agent and the support are added under specific conditions. A surfactant or a polymer is generally necessary to avoid aggregation of the nanoparticles [3]. However, in order to optimize the use of the active phase these stabilizers must be removed, which may cause agglomeration of the nanoparticles and, therefore it would be interesting to develop methodologies that avoid the use of these capping agents. With that aim, the use of a reducing agent and a metal precursor that can be employed under mild conditions to avoid the agglomeration of the nanoparticles is desirable. Organometallic precursors allow for colloidal synthesis at lower temperatures using alcohols as reducing agents, although aggregation cannot always be avoided [4]. Among these methods, the polyol process is based on the decomposition of the polyol (commonly ethylene glycol) by treatment under a certain temperature in a solution containing the metal precursor salt [5-7] to which the support can be also added [8]. In this way, Pt nanoparticles supported on carbon nanotubes (CNT) have been synthesized [9-10]. It has been suggested that the polyol acts as solvent and reducing agent [11], though an additional reducing agent is frequently needed [12-13].

The selective catalytic hydrogenation of aromatic haloamines has been extensively studied to displace the environmentally unfriendly traditional synthetic routes. Although the activation of the N=O bond is relatively easy, the main problem associated with this reaction is the accumulation of intermediates and, depending on the metal, the cleavage of the halogen. The accumulation of hydroxylamine may lead to rapid exothermic decomposition and/or formation of condensation products. The most studied metals, i.e. Ni, Pt and Pd, offer good activities for this hydrogenation, but to achieve a high yield of the desired product it might be necessary to work at high temperatures, to add promoters or to employ bimetallic catalysts [14-15]. Palladium is in general less selective than platinum for this reaction due to parallel dehalogenation, and complete inhibition of the C-Cl scission is difficult [16-17]. In

this sense it has been reported that the use of a hydrophobic support as activated carbon may inhibit the formation of aniline [17] and an alternative support as CNT can offer further improvement of the catalytic performance [18]. Moreover, recent literature points to graphene oxide as an ideal candidate to act as support for the synthesis Pd nanoparticles [19-21]. This has been achieved by chemical [22], electrochemical [23] or microwave-assisted methods [24]. Some of these methods may also reduce the parent graphene oxide in such a way that the aromatic structure is recovered.

Therefore, we have explored the synthesis of palladium nanoparticles over graphite oxide by the polyol method and compared it with the synthesis over carbon nanotubes. The catalytic performance in the hydrogenation of p-chloronitrobenzene (p-ClNB) was tested and compared with analogous catalysts prepared by conventional impregnation over GO, CNT and previously oxidized CNT.

2. EXPERIMENTAL

2.1 Catalysts preparation

Graphite oxide (GO) was synthesized from graphite powder (99.999% stated purity, 200 mesh, Alfar Aesar) following a modification of the Brodie´s method [25]. Graphite was added to a reaction flask containing fuming HNO_3 (20 mL/g of support) which was previously cooled to 273 K in an iced bath. Then, potassium chlorate (8 g/g of support) was slowly added. The reaction was left to proceed for 24 h under stirring, and the final solid was filtered, extensively washed with deionized water until neutral pH, dried under vacuum at 323 K overnight and kept in a desiccator. High purity commercial multi-wall carbon nanotubes (CNT), supplied by Nanocyl (Nanocyl 3100, > 95% purity), were also employed. A portion of the CNTs was oxidized with concentrated HNO_3 for 24 h at 403 K (CNTox). The catalysts were prepared employing the necessary amount of the precursor, palladium

acetylacetonate $Pd(acac)_2$ (Sigma Aldrich, 99%), to obtain a 1 wt.% Pd over GO and CNT. To prepare Pd/GO_{EG} and Pd/CNT_{EG} the support and the Pd precursor were dispersed in ethylene glycol and heated at 373 K for 2 h, filtered off, washed extensively with ethanol and dried under vacuum at 323 K for 16 h. Catalysts Pd/CNT, Pd/CNTox and Pd/G were prepared by incipient impregnation in toluene, followed by drying at 373 K for 24 h and heating under Ar (50 mL/min) at 673 K for 2 h, with a heating ramp of 5 ºC/min. The samples prepared by impregnation were reduced under H_2 (50 mL/min) at 673 K for 2 h prior to the reaction.

2.2 Characterization

The specific surface areas (S_{BET}) of the catalysts were determined from the N_2 adsorption isotherms at 77 K, which were obtained with a Micromeritics ASAP 2010 equipment. Prior to the measurements, the samples were degassed at 473 K for 2 h.

TEM images were obtained with a JEOL electron microscope (model JEM-2010) working at 200 kV. It was equipped with an INCA Energy TEM 100 analytical system and a SIS MegaView II camera. Samples for analysis were suspended in ethanol and placed on copper grids with a holey-carbon film support. The average particle size was obtained from the measurement of 200 nanoparticles.

X-ray powder diffraction patterns were recorded on a Rigaku diffractometer equipped with a nickel-filtered CuKα1 radiation (λ= 1.5418˚A), using a 2º/min scanning rate.

The actual Pd loading on the different catalysts was determined by ICP-OES in a Perkin-Elmer device (Optimal 3000). To this end, the metal was extracted from the catalysts by digestion in HNO_3/H_2O_2 (4:1) for 30 min, in a microwave oven at 473 K.

Thermogravimetric analyses were performed with a Mettler Toledo Thermogravimetric TGA/SDTA 851. The samples were treated under flowing He for 2 h and then heated at a 10 K/min rate up to 1123 K.

X-ray photoelectron spectra (XPS) of the catalysts were obtained on a MicrotechMultilb 3000 spectrometer, equipped with a hemispherical electron analyzer and MgKα (hν = 1253.6 eV) photon source. Prior to the analysis, the catalysts were in situ reduced under the same conditions employed before the catalytic tests. The surface O/C and Pd/C atomic ratios were estimated from the integrated intensities of Pd $3d_{5/2}$, C 1s, and O 1s lines after background subtraction and correction by the atomic sensitivity factors. The spectra were fitted to a combination of Gaussian–Lorentzian lines of variable proportions.

Infrared spectra were collected on a NicoletNexus FT-IR in the middle range (4000 – 400 cm^{-1}), and recorded by a DTGS detector from 128 scans and with a resolution of 4 cm^{-1}. GO and its derivatives were mixed with pre-dried potassium bromide to a final concentration of approximately 1% (w/w).

2.3 Hydrogenation tests

Catalytic tests were performed in a stainless steel Parr-type batch reactor, equipped with a glass sleeve and a magnetic stirrer set at 1000 rpm. The hydrogenations were performed with 50 mg of catalyst, 320 mg of p-chloronitrobenzene and 50 mL of ethanol were stirred at 20 bar and 298 K. For the recycling studies the amounts were recalculated for each cycle. The concentrations of reactants and products were monitored by gas chromatography mass spectrometry using a GC–MS instrument (Shimadzu GCMS-QP5050) with chiral β-Dex 225, a 30-m column (Supelco), and He as the carrier gas. Additional experiments were performed to verify whether the reaction was heterogeneously

catalyzed: the reaction was stopped at 50% conversion and the liquid filtrate was submitted to the reaction conditions.

3. Results

3.1 Characterization

The estimated BET surface areas are reported in Table 1. It can be seen that the surface area of the supports slightly decreased after the incorporation of Pd. On the other hand, the BET surface area of Pd/G was much higher, 670 $m^2 \cdot g^{-1}$ as a consequence of the expansion of the GO layers during the thermal exfoliation treatment applied in the synthesis of this catalyst. The adsorption isotherms of samples GO and Pd/GO_{EG} could not be measured because the pretreatment changed the structure of the support, as it was verified by XRD analysis performed after the adsorption experiment.

Fig. 1 shows representative TEM images of the catalysts. It can be observed that Pd/GO_{EG}, Fig. 1a, presented transparent areas corresponding to exfoliated graphene sheets, along with zones where the sheets seemed to be thicker. However, sample Pd/G, Fig. 1b, was less homogeneous and, although it also displayed some exfoliated areas, a high proportion of the images showed dark regions that resembled amorphous carbon. From these images it can be concluded that palladium nanoparticles densely covered the surface in Pd/G and Pd/GO_{EG} catalysts Pd nanoparticles on Pd/GO_{EG} were mostly smaller than 2 nm, and they could not be properly measured, although some particles of around 8-10 nm could also be observed. On the other hand, sample Pd/G displayed a heterogeneous particle size distribution with an estimated average size of 4.1 nm. For the CNT-based catalysts different nanoparticle sizes distribution was also found, and the average particle size, reported in Table 1, followed the trend Pd/CNT_{EG} < Pd/CNTox < Pd/CNT. On catalyst Pd/CNT, Fig. 1d, the nanoparticles mainly formed large agglomerates, the estimated average particle size being 9.4 nm. The surface of catalysts Pd/CNT_{EG} and Pd/CNTox was more homogeneously

covered with Pd nanoparticles, the mean metal particle size for Pd/CNTox was 2.7 nm. The particle sizes obtained for Pd/GO_{EG} and Pd/CNT_{EG} were the smallest among the prepared catalysts, in the range of previously reported values in literature for Pd nanoparticles (1.6 wt.%) supported on graphene and graphene oxide [14], and smaller than the values reported for non-supported palladium nanoparticles stabilized by an organic moiety [26].

The XRD patterns of GO and GO-based catalysts are shown in Fig. 2. The position and wideness of the diffraction peaks provide an estimation of the crystallinity an exfoliation of these laminar materials. For the sample GO, the intense and sharp peak of the (001) reflection centered at $2\theta = 15.4°$ corresponding to an interlayer distance of 0.57 nm, and the disappearance of the peak at 26º due to the reflection of the (002) of graphite confirm a high yield in the GO synthesis [27]. The synthesis of palladium nanoparticles over GO afforded new materials with different morphology, as their XRD profile showed. The sample Pd/GO_{EG} displayed a new diffraction peak at $2\theta = 11.2º$ and a wider peak centered at 2θ ~22°. The diffraction peak at lower angle indicates that the material was partially exfoliated, the new interlayer distance being 0.79 nm. The exfoliated layers could be filled with palladium nanoparticles or residues of ethylene glycol. The broader peak could be an indication of the presence of graphene layers with different interlayer distance, which could be turbostratic graphite as some TEM images suggested [28-29]. On the other hand, for sample Pd/G the characteristic peak of GO disappeared and it displayed the broad peak at 2θ ~22°, which is ascribed to turbostratic graphite. The XRD profiles of the GO-based catalysts corroborate the TEM observations, which suggested that Pd/GO_{EG} was more exfoliated than Pd/G. The XRD of CNT-based catalyst (not shown) displayed the characteristic peak of graphite at $2\theta = 26º$, wider than the one observed for graphite as a result of the rolling structure. Finally, none of the diffractograms showed the characteristics

peaks of palladium or its oxide, probably because of the low percentage of metal on the samples and/or to the small particle size.

The thermogravimetric analyses (Fig.3) were performed to study the thermal stability of the samples and the presence of organic residues. The thermogram of GO showed a main weight loss with maximum rate at 534 K, which corresponds to the release of H_2O, CO and CO_2 during the reductive exfoliation [26]. The weight loss of this stage was 25%. At higher temperatures, the weight loss followed a slower rate and a total mass loss of about 46% was reached. The weight loss and the temperature at which it was produced were similar to others reported for GO prepared by this method [26][30]. The thermogravimetric profile of Pd/GO_{EG} was shifted to lower degradation temperature, 489 K, and the weight loss at this stage was similar to that of GO. The presence of ethylene glycol molecules inside the layers may be responsible of the lower thermal stability, as previously reported for other solvents [31], and it would be in agreement with the XRD results that showed an increase in the interlayer distance. Furthermore, modifications on the type of solvent-GO interaction during the thermal analysis could be responsible for the degradation of the solvent molecules at higher temperature (>523 K), and it would explain the increase of the weight loss at this stage compared to GO. The thermogram of Pd/G showed much higher thermal stability with barely any mass loss until 655 K, which was followed by a smoother decay up to 29 % of total weight loss. Nonetheless, the high total weight loss observed for Pd/G compared to Pd/CNT suggested that there is a large proportion of carbon on defects on this sample, as observed by TEM and XRD. The thermal analyses of the CNTs and their corresponding catalysts are shown in Fig. 3b. It can be observed that the Pd/CNT catalyst showed barely any mass loss along the whole range of temperature. On the contrary, catalysts Pd/CNTox and Pd/CNT_{EG} displayed a total mass loss of 10 and 12 % respectively, which can be ascribed

to the decomposition of the oxygen groups that are present after the reduction treatment and the degradation of adsorbed ethylene glycol, respectively.

Infrared spectra of GO and the GO-based catalysts are shown in the supplementary information, Fig. S1. GO displayed the characteristic bands of C-OH groups at 3627, 3490, 1620 and 1383 cm^{-1} [28][32-33], C=O bond of carbonyl and/or carboxyl at 1713 cm^{-1} and the band at 1063 cm^{-1} due to deformation of the C-O bond of epoxy functionalities. The infrared spectra of the sample Pd/GO_{EG} showed a decrease of the bands at 3627, 3490, 1713 and 1620 cm^{-1}, while new bands appeared at 2930 and 2853 cm^{-1} assigned to asymmetric and symmetric stretching vibration of CH_2 group and to the vibration of C sp^2-C sp^2 respectively, and a small band at 1562 cm^{-1} assigned to the vibration of C sp^2-Csp^2 bonds characteristic of the skeletal vibrations of graphitic domains. These changes point to the contribution of ethylene glycol molecules on the Pd/GO_{EG} catalyst by reaction with the hydroxyl groups on the parent GO, in agreement with the XRD profiles and the thermal analysis, and to the partial recovery of the aromaticity. On the other hand, sample Pd/G displayed the band at 1578 cm^{-1} ascribed to the vibration of C sp^2-C sp^2 bonds, which confirms the reduction of this material. In addition, qualitative changes could be observed for sample Pd/G in the low frequency range, which also suggest modifications on the surface chemistry.

Analyses of the XPS spectra of the catalysts were performed. The detailed values for the C 1s and O 1s regions and their proportions, which are included in the supporting information, are in quite good agreement with literature [27-28] [34]. The C 1s and O1s region of GO and the GO-based catalysts are shown in Fig. 4a and 4c. As expected, the position of the maximum of the C 1s spectra for GO appears at higher B.E, 286.0 eV, than the corresponding to graphite which is ascribed to sp^2 carbon atoms, i.e. 284.6 eV, and the characteristic $\pi \rightarrow \pi^*$ peak of polyaromatic structures is absent. This confirms that the main

contribution is associated to sp^3 carbon atoms. The C 1s spectra of Pd/GO_{EG} slightly changed compared to that for GO, but the proportion of the contribution ascribed to sp^2 carbon is higher than for GO, in agreement with the IR spectra. On the other hand, for catalyst Pd/G the contribution of sp^3 carbon has clearly decreased, this indicating that the support in Pd/G recovered the aromaticity. As far as the O 1s region is concerned, the maximum for GO was at 532.0 eV and it displayed the contribution of three components assigned to oxygen in carbonyl groups (531.2 eV), oxygen atoms in C-O bonds like hydroxyl and ether groups (532.6 eV) and oxygen atoms in acidic carboxyl groups (533.5 eV). The maximum of the O 1s peaks was shifted to higher binding energies for the Pd/G and Pd/GO_{EG} catalysts compared to GO, 532.7-533.6 eV, this clearly indicating a change in the chemical state of the oxygen species. For the catalyst Pd/GO_{EG}, bearing in mind the thermal analysis and the XRD profile that suggested the presence of intercalated solvent, it seems plausible that the hydroxyl groups of the support had reacted with the hydroxyl groups of the solvent molecules *via* hydrogen bond or condensation, as observed when other molecules were intercalated within the layers, and this would explain the more oxidized state of oxygen on these samples [27] [35]. The C 1s region of CNT displayed the maximum at 284.6 eV ascribed to sp^2 carbon, and the typical contributions of carbon materials. No significant changes were observed for the C 1s region of the CNT-based catalysts. The O 1s region of CNT and CNTox displayed the contributions ascribed to oxygen in carbonyl groups (531.6-531.7eV), oxygen atoms in C-O bonds (533.1-533.2 eV) and oxygen atoms in acidic carboxyl groups (534.5-534.7 eV). It was observed that the contribtion ascribed to carboxylic acid increased upon the oxidation treatment, and then it decreases for the Pd/CNTox catalyst. For catalysts Pd/CNT_{EG} and Pd/CNT no significant differences were observed in the relative contributions of each component. The relative amounts of C, O and Pd were calculated from the corresponding peak areas divided by the sensitivity factors, and the most relevant data

are shown in Table 1. It was observed that the O/C ratio for sample Pd/GO_{EG} (Table 1) increased compared to GO, which confirms the presence of remaining solvent molecules in this material, as other characterization results showed. Opposite to this, the O/C ratio decreased for Pd/G compared to GO, in agreement with the infrared spectrum and the thermal analysis. The O/C ratio for Pd/CNT was lower compared to Pd/CNTox and Pd/CNT_{EG}, which confirms that these latter catalysts presented oxygen groups and ethylene glycol, respectively, on the surface as the thermal analyses suggested. Moreover, all the catalysts displayed a new peak around 335 eV corresponding to the Pd $3d_{5/2}$ level (Supporting Information, Fig. S2), and the BEs values are shown in Table 1. It is important to remark that the deconvolution of this region displayed only one contribution ascribed to Pd^0 for all the catalysts except Pd/G, despite the mild conditions employed for the synthesis of the nanoparticles on Pd/GO_{EG} and Pd/CNT_{EG}. For the Pd/G catalyst two components have to be considered at 335.4 and 337.7 eV, which are ascribed to Pd^0 and Pd^{+2} respectively [36-37]. The contribution of each component is also included in brackets in Table 1, and it indicates that palladium was reduced to a larger extent. The Pd/C ratio was also estimated and the values are shown in Table 1. Most of the samples displayed a Pd/C ratio in the range 0.001-0.002 except for Pd/CNTox, with a ratio of 0.007. Considering the superficial character of the XPS technique and the ICP analyses in Table 1, the higher surface Pd/C ratio for this sample compared to Pd/CNT would be in line with the smaller palladium particle size obtained in Pd/CNTox, as observed by TEM. On the other hand, the similar Pd/C ratio for catalyst Pd/CNT_{EG} compared to Pd/CNT, despite the higher dispersion of Pd nanoparticles on Pd/CNT_{EG}, can be explained by its lower content on Pd, and similar conclusions can be made for the Pd/C ratio of catalysts Pd/G and Pd/GO_{EG}. However, as the TEM images suggested, it is plausible to consider that a proportion of the palladium oxide is encapsulated in the carbon structure for the Pd/G catalyst, and this could also explain the

similar Pd/C ratio compared to Pd/CNT and the lower reduction degree of this sample, as less particles would be accessible to the hydrogen reduction flow.

3.2 Reaction

The catalysts were tested in the liquid phase hydrogenation of p-chloronitrobenzene. The evolution of the conversion *vs* time is shown in Fig. 5a and the most relevant results are shown in Table 2. All the catalysts were active, and the activity calculated as mol of p-ClNB converted per mol of Pd (obtained from ICP-OES) and reaction time at 50% conversion in the first cycle followed the trend Pd/CNT_{EG} > Pd/CNTox > Pd/GO_{EG} > Pd/CNT >> Pd/G. The activity achieved with Pd/GO_{EG} and Pd/CNT was in the range of the values reported for palladium supported over activated carbon, while those obtained with Pd/CNTox and Pd/CNT_{EG} were nearly one order of magnitude higher [17]. As far as the selectivity is concerned, p-ClAN was the main product of the reaction for all the catalysts and, under the experimental conditions employed, no intermediates were observed. The selectivity to p-ClAN was 100% with all the catalysts except for Pd/CNTox, which afforded a selectivity of 78% when 100% conversion was reached, the secondary product being exclusively aniline (AN). In addition, the stability of Pd/CNT_{EG}, and Pd/GO_{EG} was studied by re-using the catalysts in three cycles, and the evolution of the conversion with time on stream is shown in Fig. 5b and 5c, respectively. The activity decreased in the second cycle, this decrease being more pronounced for Pd/GO_{EG} (70 %) than for Pd/CNT_{EG} (44%). However, the activity was stable in the third cycle for both catalysts, and the selectivity to p-ClAN remained 100% upon recycling within the conversion range. Additional experiments, described in the Experimental Section, were performed with catalysts Pd/CNT_{EG} and Pd/GO_{EG} to assess that the reaction was heterogeneously catalysed. The

absent of reaction with the liquid filtrate confirmed that the reaction was heterogeneously catalysed despite the possible leaching of palladium nanoparticles.

The hydrogenation paths of p-ClNB are summarized on Scheme 1. The catalytic reduction of p-ClNB may proceed through the hydrogenation of the nitro group to give the desired product p-ClAN. Then, p-ClAN may suffer dehalogenation to produce AN. The dehalogenation may also take place on the p-ClNB molecule producing nitrobenzene (NB) which could then be hydrogenated to AN [15]. It has been suggested that the dehalogenation reaction occurs via electrophilic attack of the activated hydrogen on the absorbed aromatic halides [38].

The obtained results reflect the influence of the synthesis method and surface chemistry of the support on the activity and selectivity in this reaction. On one hand, the activity achieved with Pd/CNTox was higher than that obtained with Pd/CNT, as well as the calculated intrinsic activity considering the palladium dispersion estimated by TEM. It has been proposed in the literature that the hydroxyl groups of the support interact with the nitro groups of the reactant, this activating the N=O bond [39]. Alternatively, it has been proposed that the electron rich acid groups of the surface may be the adsorption sites for the aromatic ring, this increasing the activity [40].

Concerning the selectivity it is interesting to remark the high value obtained with Pd/CNT, as Pd has been generally considered as a non-selective metal for p-ClNB hydrogenation due to the formation of AN. For that reason, it has been employed in combination with other elements, either by forming bimetallic catalyst (Pd/Au and Pd/Ni supported on alumina [41][15]) or by the use of additives in the reaction medium [42]. Apparently, the addition of a second metal activates the N=O bond and hinders the adsorption of the p-ClAN avoiding its subsequence dehalogenation. However, in the case of carbon nanotubes, the π cloud of the support may repel the Cl atom, this favoring an increase of selectivity [43], similarly to what

has been observed in the hydrogenation of cinnamaldehyde [44]. Moreover, the oxygen groups on the catalyst surface, which are present on Pd/CNTox even after the reduction treatment, may favor the adsorption of the formed p-ClAN on the support and this would enable its consecutive dehalogenation [39]. Therefore, the presence of oxygen groups on the surface seems to favor the activity while diminishes the selectivity.

It has been observed that Pd nanoparticles in Pd/CNT_{EG} and Pd/GO_{EG} displayed similar particle size, this suggesting that the morphology and surface chemistry do not affect the size of the nanoparticles obtained by this methodology. Nonetheless the activity was higher when the catalyst Pd/CNT_{EG} was employed, which can tentatively be related to its higher surface area. Unfortunately, the specific surface area of Pd/GO_{EG} could not be properly measured, as explained in Section 3.1. These structural changes upon heating can be explained considering that the exfoliated structure is preserved due to the intercalated ethylene glycol, which seem to be decomposed already at the pretreatment temperature of the adsorption isotherm analysis. Furthermore, both catalysts displayed high selectivity to p-ClAN. The high selectivity obtained with Pd/GO_{EG}, along with the characterization results, confirms the proposed chemical interaction between the surface OH and the ethylene glycol molecules. This would avoid the interaction between the surface oxygen groups which, according to the characterization results, are present on the Pd/GO_{EG} catalyst, and the reactant molecules and, thus, hinder the formation of aniline, the undesired product. In addition, the Pd/CNT_{EG} and Pd/GO_{EG} catalysts proved to have good recyclability after the first cycle. The loss of activity observed between the first and the second cycle might be due to the leaching of adsorbed Pd nanoparticles as the Pd/C ratio of the fresh and the used catalysts obtained by XPS showed. The conversion profiles in the second and third cycle seem to display an induction period for both Pd/CNT_{EG} and Pd/GO_{EG}, which might be due to the progressive reduction of the palladium oxide layer under the reaction conditions [19]. The similar O/C ratio in the used

Pd/GO_{EG} catalyst and in the fresh one seems to confirm the above mentioned chemical interaction between ethylene glycol and the oxygen groups on the surface of GO which avoids the desorption of the ethylene glycol, unlike to what is observed for the used Pd/CNT_{EG} catalyst, for which the O/C ratio is lower than in the fresh catalyst.

Finally, the activity achieved with the Pd/G catalyst was much lower than that obtained with Pd/CNT, despite the higher surface area on the former. For this sample the characterization studies suggested that Pd was not fully reduced, and that a given amount of the Pd nanoparticles may be encapsulated inside the carbon structure and, therefore, they might not be accessible to reactants. In the literature, the synthesis of metal nanoparticles supported on graphene oxide by impregnation followed by heating under air or nitrogen flow has been reported for Pd, Pt, Ru, Au or Ag among others metals. Those catalysts were active, however no comparison with other systems was made and the metal loading was higher than that employed in the present work, i.e. 10-25 wt.% [45-46]. Alternatively, the impregnation could have been performed before the reduction of GO but, in that case, the inert surface may also lead to low dispersion.

4. Conclusions

We have synthetized Pd nanoparticles over CNT and GO employing ethylene glycol as reducing agent, and compared their catalytic performance in the chemoselective hydrogenation of p-ClNB with analogous catalysts prepared by traditional impregnation and over previously oxidized CNT. The characterization studies showed that the polyol method was effective for obtaining metal palladium nanoparticles over CNT and GO, and the catalysts Pd/CNT_{EG} and Pd/GO_{EG} displayed similar Pd particle size which was smaller than those obtained by the traditional impregnation method. The characterization performed

seems to indicate that under the synthesis conditions employed, ethylene glycol reacted with the oxygen groups of the parent GO surface and, thus, Pd/GO_{EG} holds intercalated solvent. Also, according to the characterization studies, a given amount of the Pd precursor and/or the Pd oxide was encapsulated inside the structure of the reduced graphene oxide in the catalyst prepared by impregnation over GO, Pd/G. This may hinder the accessibility of H_2 making more difficult the reduction of palladium oxide.

The catalysts were tested in the chemoselective hydrogenation of p-ClNB. It was observed that the activity was higher over Pd/CNTox catalyst than over Pd/CNT, what can be ascribed to the presence of oxygen groups on the Pd/CNTox surface. However the selectivity to the desired halo-aniline, p-ClAN, was lower over Pd/CNTox, and this has been explained also by the presence of oxygen groups on the surface. On the other hand, it was found that Pd/CNT_{EG} was more active than $Pd/GO_{EG,}$ which can be due the different surface area. The passivation of the oxygen groups on the Pd/GO_{EG} surface by molecules of ethylene glycol seem to favor the selectivity of this catalyst. The traditional impregnation of the metallic precursor over GO followed by hydrogen reduction under heating hinders the reduction of palladium oxide and promotes the encapsulation of palladium oxide and/or palladium precursor, this leading to a less active catalyst. Finally the stability of both Pd/CNT_{EG} and Pd/GO_{EG} was proved after an initial loss of activity due to the partial leaching of Pd nanoparticles.

In summary, the oxygen groups on the surface of the support were found to be detrimental for the selectivity. However, as observed by TEM, the dispersion of the metal nanoparticles was improved. In order to increase the dispersion of palladium without performing the oxidation of the surface the synthesis of nanoparticles can be performed by reduction with ethylene glycol, this avoiding the previous oxidation step.

Acknowledgements

Financial support for the present study was received from CONICYT Chile, project 3130483 (Postdoctoral), Generalitat Valenciana, Spain (PROMETEOII/2014/004) is also gratefully acknowledged.

References

[1] S.I. El-Hout, S.M. El-Sheikh, H.M.A. Hassan, F.A. Harraz, I.A. Ibrahim, E.A. El-Sharkawy, Appl.Catal. A: General 503 (2015) 176–185.

[2] N. Marín-Astorga, G. Alvez-Manoli, P. Reyes, J. Mol. Cat. A: Chem. 226 (2005) 81–88.

[3] M.L. Toebes, J.A. van Dillen, K. P. de Jong, J. Mol. Cat. A: Chem. 173 (2001) 75-98.

[4] J. Athilakshmi, S. Ramanathan, D.K. Chand, Tetrahed. Lett. 49 (2008) 5286–5288.

[5] L.K. Kurihara, G.M. Chow, P.E. Schoen, NanoStruct. Mater. 5 (1995) 607-613.

[6] F.A. Harraz S.E. El-Hout, H.M. Killa, I.A. Ibrahim, J. Catal. 286 (2012) 184–192.

[7] I.S. Armadi, Z.L.Wang, T.C. Green, A. Henglein, M.A.E. Sayed, Science 272 (1996) 1924-1925.

[8] A. Miyazaki, I. Balint, K.I. Aika, Y. Nakano, J. Catal. 203 (2001) 364.

[9] V. Lordi, N. Yao, J. Wei, Chem. Mater. 13 (2001) 733-737.

[10] W.Z. Li, C.H. Liang, J.S. Qiu, W.J. Zhou, H.M. Han, Z.B. Wei, G.Q. Sun, Q. Xin, Carbon 40 (2002) 791-794.

[11] L.K. Kurihara, G.M. Chow, P.E. Schoen, NanoStruct. Mater. 5 (1995) 607-613.

[12] C.C Yeh, D.H. Chen, Appl. Catal. B: Environ. 150– 151 (2014) 298– 304.

[13] H.T. Zhu, C.Y.Zhang, Y.S. Yin, J. Cryst. Growth 270 (2004) 722–728.

[14] H.U. Blaser, A. Schnyder, H. Steiner, F. Rössler, P. Baumeister in Handbook of Heterogeneous Catalysis (Wiley, 2008), vol. 8 pp. 3284-3307

[15] F. Cárdenas-Lizana, S. Gómez-Quero, C. Amorim, M.A. Keane, Appl. Catal. A: General 473 (2014) 41–50.

[16] H. Liu, M.Liang, C. Xiao, N. Zheng, X. Feng, Y. Liu, J. Xie, Y.Wang J. Mol. Catal. A: General 308 (2009) 79-86.

[17] V. Krathy, M. Kralik, M. Mecarova, M. Stolcova, L. Zalibera, M. Hronec, Appl. Catal. A, 235 (2002) 225-231-

[18] A.B. Dongil, C. Rivera-Cárcamo, L. Pastor-Pérez, A. Sepúlveda-Escribano, P.Reyes, Catal. Today, 249 (2015) 72-78.

[19] K.H.Lee, S.W.Han, K.Y. Kwon, J. B. Park, J. Coll. Interf. Sci 403 (2013) 127–133.

[20] R. Awasthi, R.N. Singh, Carbon 51 (2013) 282 –289.

[21] X. Chen, G.Wu, J.Chen, X. Chen, Z. Xie, X. Wang, J. Am. Chem. Soc. 133 (2011) 3693–3695

[22] Á. Mastalir, Z. Király, Á. Patzkó, I. Dékány, P. L'Argentiere, Carbon 46 (2008) 1631-1637.

[23] Y. Wang, Y. Zhao, J.Yin, M. Liu, Q. Dong, Y. Su, Int. J. Hydrogen Energy 39 (2014) 1325-1335.

[24] A.R. Siamaki, Abd El Rahman S. Khder, V.Abdelsayed, M. Samy El-Shall, B. Frank Gupton J. Catal. 279 (2011) 1–11.

[25] A.B.Dongil, B.Bachiller-Baeza, A. Guerrero-Ruiz, I.Rodríguez-Ramos, Catal. Comm. 26 (2012) 149-154.

[26] S.Jansat, M. Gómez , K. Philippot , G. Muller , E.Guiu ,C. Claver, S.Castillón, B.Chaudret, J. Am. Chem. Soc., 126 (2004) 1592–1593.

[27] A.B. Dongil, B. Bachiller-Baeza, A. Guerrero-Ruiz, I. Rodríguez-Ramos, J. Catal. 282 (2011) 299-309.

[28] Z.Q. Li, C.J. Lu, Z.P. Xia, Y. Zhou, Z. Luo, Carbon 45 (2007) 1686-1695.

[29] A.B. Bourlinos, D. Gournis, D. Petridis, T. Szabo, A. Szeri, I. Dekany, Langmuir, 19 (2003) 6050-6055.

[30] F. Barroso-Bujans, S. Cerveny, R. Verdejo, J.J. del Val, J.M. Alberdi, A. Alegría, J. Colmenero, Carbon 48 (2010) 1079–1087.

[31] F. Barroso-Bujans, J.L. G. Fierro, A. Alegría, J.Colmenero, Thermochim. Acta 526 (2011) 65– 71.

[32] M. Mermoux, Y. Chabre, A. Rousseau, Carbon 29 (1991) 469-474.

[33] T. Szabó, O. Berkesi, P. Forgó, K. Josepovits, Y. Sanakis, D. Petridis, and I. Dékény, Chem. Mater. 18 (2006) 2740.

[34] N.I.Kovtyukhova, P.J. Olliver, B.R. Martin, T.E. Mallouk, S.A. Chizhik, E.V. Buzaneva, A.D. Gorchinskiy, Chem. Mater. 11 (1998) 771-778

[35] Y.Matsuo, Y.Sakai, T. Fukutsuka, Y.Sugie, Carbon 47 (2009) 804–811.

[36] J.C Hierso, C.Satto, R. Feurer, P. Kalck, Chem Mater 8 (1996) 2481-2485.

[37] W.Sun, X.Lu, Y. Tong, Z. Zhang, J.Lei, G.Nie, C.Wang, Int. J. Hydrogen Energy 39 (2014) 9080–9086.

[38] F. Notheisz, M. Bartok, in Fine Chemicals Through Heterogeneous Catalysis (Wiley 2001) New York, 415-426.

[39] A. Nieto-Marquez, S. Gil, A. Romero, J. L.Valverde, S. Gómez-Quero, M.A. Keane, Appl. Catal. A: General 363 (2009) 188–198.

[40] M. V.Rahaman, M. A. Vannice, J. Catal. 127 (1991) 267-275.

[41] F. Cardenas-Lizana, S. Gomez-Quero, A. Hugon, L. Delannoy, C. Louis, M. A. Keane J. Catal. 262 (2009) 235‑243.

[42] Q.Xu, X.M. Liu, J.R. Chen, R.X. Li, X.J. Li, J. Mol. Catal. A: Chemical 260 (2006) 299–305.

[43] N. Mahata, A.F. Cunha, J.J.M. Órfão, J.L. Figueiredo, Catal. Comm 10 (2009) 1203-1206.

[44] J.P. Tessonnier, L. Pesant, G. Ehret, M. J. Ledoux, C. P.Huu, Appl. Catal. A: General 288 (2005) 203–210.

[45] K.Gotoh, K. Kawabata, E. Fujii, K. Morishige, T. Kinumoto, Y. Miyazaki, H. Ishida, Carbon 47 (2009) 2112-2142.

[46] K. Gotoh, T.Kinumoto, E. Fujii, A. Yamamoto, H. Hashimoto, T. Ohkubo, A. Itadani, Y. Kuroda, Hiroyuki Ishida, Carbon 49 (2011) 1118-1125.

Figure 1. TEM micrographs of a) Pd/GO_{EG} ; b) Pd/G; c) $Pd/CNT_{EG;}$ d) Pd/CNT; e) Pd/CNTox.

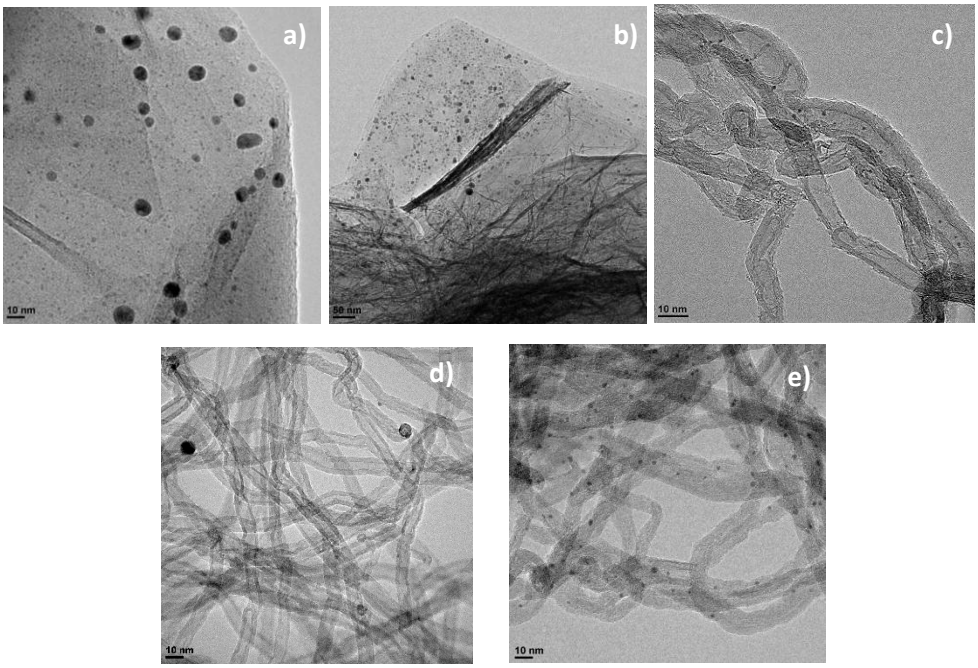

Figure 2. XRD patterns of the GO-based catalysts.

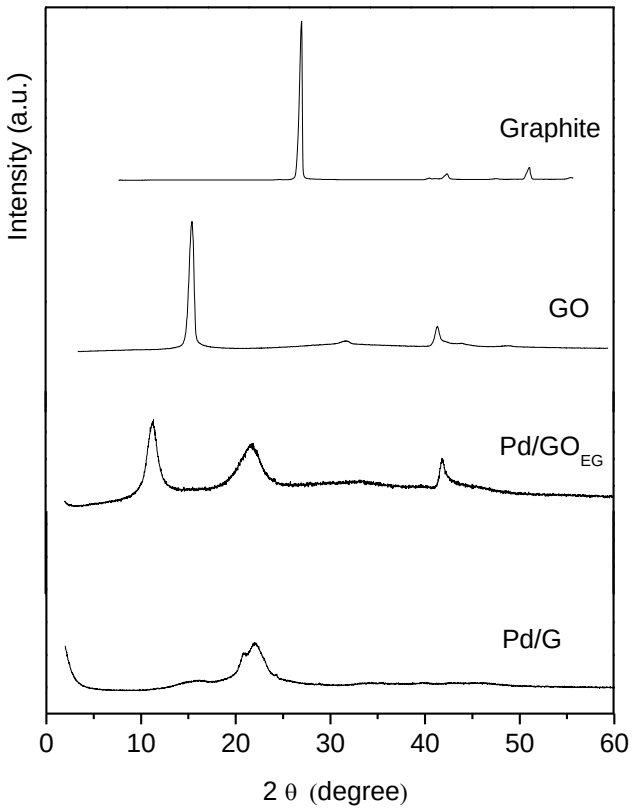

Figure 3. Thermal analyses of the a) GO (—), Pd/GO_{EG} (·····), Pd/G (—) and b) Pd/CNT (—), Pd/CNTox (—) and Pd/CNT_{EG} (·····).

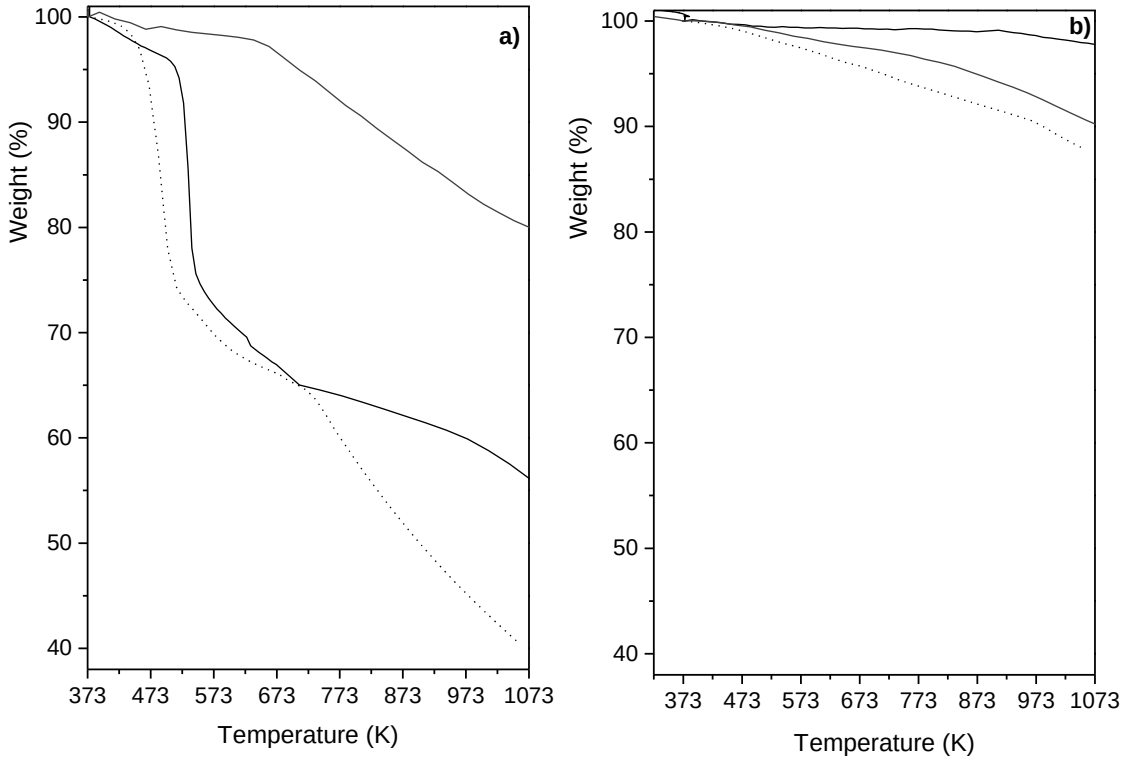

Figure 4. XPS spectra of the C 1s region a) GO and GO-based catalysts; b) CNT, CNTox and CNT-based catalysts and the O 1s region c) GO and GO-based catalysts, d) CNT, CNTox and CNT-based catalysts.

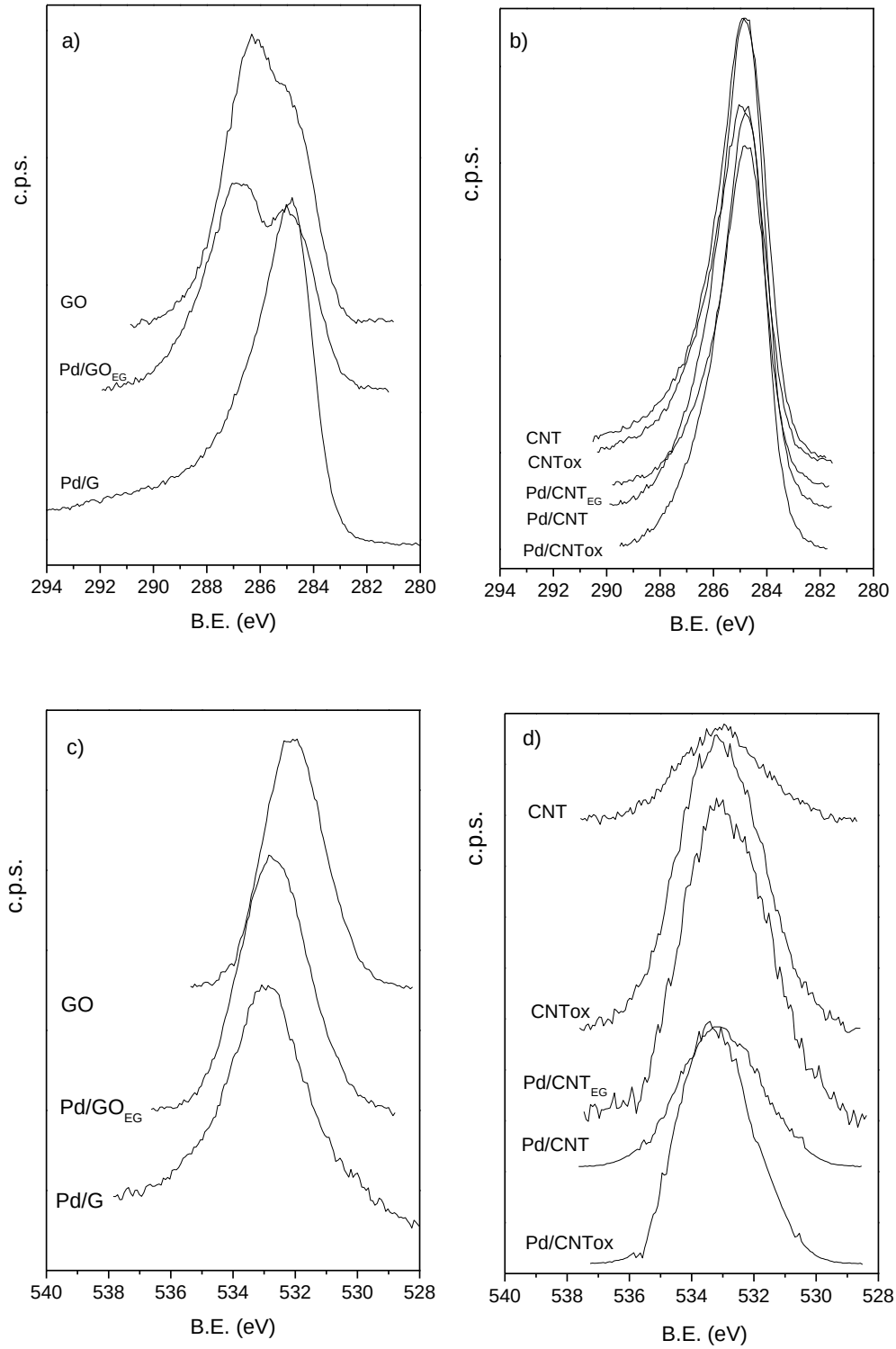

Figure 5. Conversion of p-cloronitrobenzene *vs* time a) First cycle; b) Pd/CNT_{EG} and c) Pd/GO_{EG} on successive cycles.

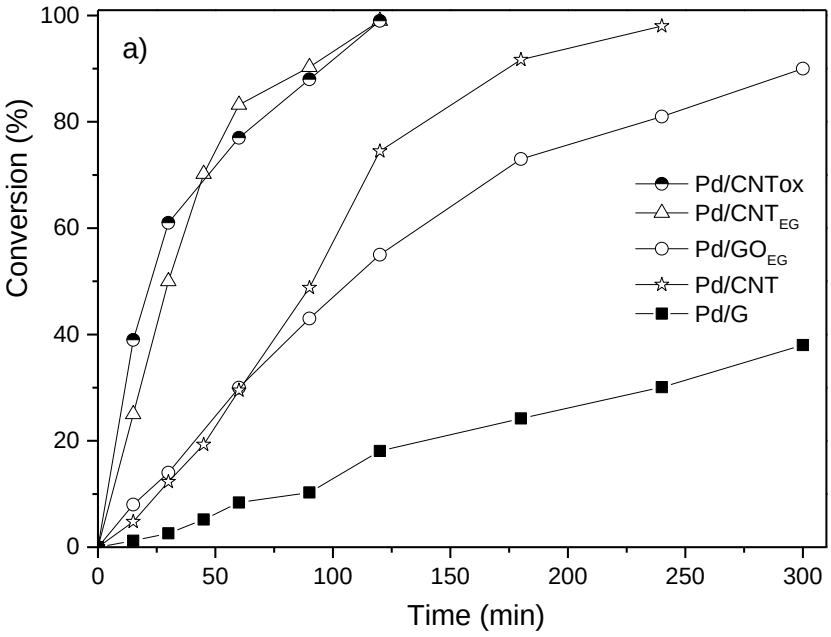

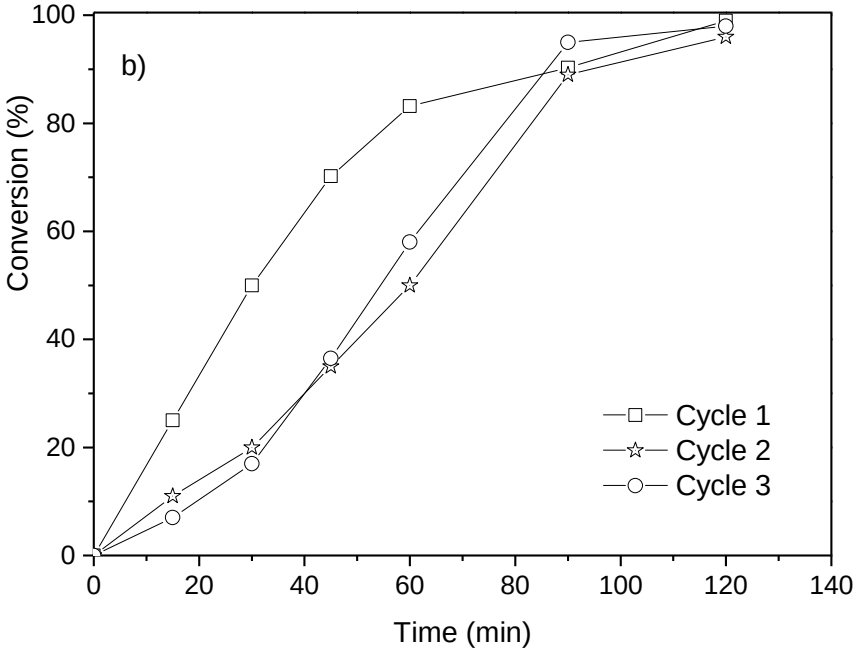

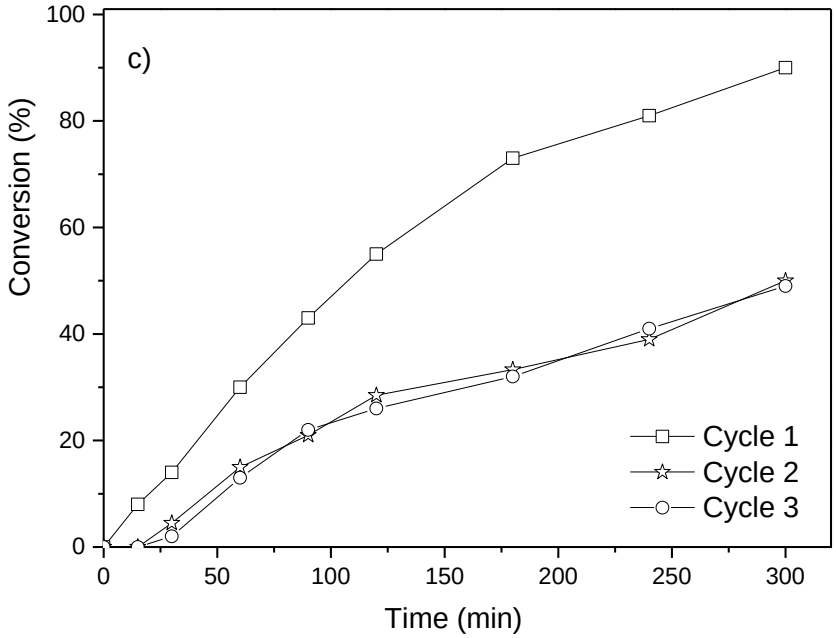

Scheme 1. Reaction paths for the para-chloronitrobenzene hydrogenation.

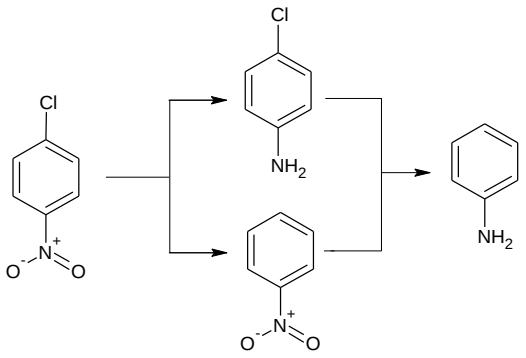

Table 1. Physico-chemical properties of supports and catalysts.

Sample	**S_{BET} ($m^2 \cdot g^{-1}$)**	**dp TEM (nm)**	**Pd $3d_{5/2}$ eV**	**O/C**	**Pd/C**	**Pd (%) ICP**
GO	-	-	-	0.355	-	-
CNT	300	-	-	0.011	-	-
CNTox	319	-	-	0.088	-	-
Pd/GO_{EG}	-	< 2	335.1	0.474	0.002	0.62
Pd/GO_{EG}- used	-	-	335.2	0.455	0.001	-
Pd/G	670	4.1	335.4 (73) 337.1 (27)	0.084	0.002	0.90
Pd/CNT_{EG}	288	< 2	335.2	0.096	0.002	0.51
Pd/CNT_{EG}- used	-	-	335.2	0.029	0.001	-
Pd/CNT	285	9.4	335.9	0.022	0.001	1.02
Pd/CNTox	289	2.7	335.7	0.071	0.007	0.91

Table 2. Catalytic activity.

Sample	**Cycle**	**Activity (min^{-1})[a]**	**% AN at max. conversion**
Pd/GO_{EG}	1	27	0
	2	8	0
	3	8	0
Pd/G	1	3[b]	0
Pd/CNT_{EG}	1	124	0
	2	69	0
	3	69	0
Pd/CNT	1	11 (92)[c]	0
Pd/CNTox	1	63 (152)[c]	22

[a] Estimated as mol of p-ClNB converted per mol of Pd (from ICP analyses) and reaction time for 50% conversion.
[b] Estimated at 40 % conversion.
[c] Intrinsic activity in brackets, estimated as Activity/Dispersion; (Dispersion $_{Pd}$= $1.12/d_p$).